Journal of Environmental Chemical Engineering 7 (2019) 102909

Contents lists available at ScienceDirect

Journal of Environmental Chemical Engineering

journal homepage: www.elsevier.com/locate/jece

Adsorptive removal of Cr(VI) from simulated wastewater in MOF **BUC-17** ultrafine powder

Jie Guo[a], Jun-Jiao Li[b], Chong-Chen Wang[a,*]

[a] Beijing Key Laboratory of Functional Materials for Building Structure and Environment Remediation, Beijing University of Civil Engineering and Architecture, Beijing, 100044, China

[b] China Aviation Planning and Design Institute (Group) CO., LTD., Beijing, 100028, China

ARTICLE INFO

Keywords:
BUC-17
Ultrafine powder
Cr(VI)
Adsorption
Mechanism

ABSTRACT

A water-stable metal-organic framework $[Co_3(tib)_2(H_2O)_{12}](SO_4)_3$ (**BUC-17**) with 2D graphene-like crystal structure was tuned to produce ultrafine powder via the introduction of absolute ethanol. The **BUC-17** powders were further characterized by powder X-ray diffraction (PXRD), scanning electron microscopy (SEM), X-ray photoelectron spectroscopy (XPS) and Zeta potential analysis. The **BUC-17** ultrafine powder exhibited excellent adsorption performance toward Cr(VI) from simulated wastewater, in which the maximum uptake capacity is 121 mg g^{-1} at pH = 4. The kinetics fitting results revealed that the adsorption process is more suitably described by the pseudo-second-order kinetics model. The negative standard free energy change ΔG°, positive enthalpy change ΔH°, and positive entropy change ΔS° of the adsorption process implied that the adsorption between **BUC-17** and Cr(VI) was spontaneous and endothermal. As well, the influencing factors of the adsorption process like pH, adsorbent dosage, initial concentration and foreign ions were investigated. Finally, the adsorption mechanism of **BUC-17** toward Cr(VI) was proposed.

1. Introduction

Chromium exists frequently as the trivalent (Cr(III)) or hexavalent (Cr(VI)) forms in aqueous systems. Chromium of different oxidation states display different characteristics in terms of potential toxic impact on human or biological organisms [1,2]. It is well known that Cr(VI) is considerably more toxic than Cr(III) [3]. In fact, the Cr(III) is considered to be as an essential trace metal nutrient for human being, whereas the Cr(VI) has been reported to be a primary contaminant to humans and other species due to its carcinogenic and durable properties [4]. Most chromium in the environment is mainly discharged from industrial procedures including but not limited to electroplating, leather, textile preservation, and metal processing [5]. Thus, National Environmental Protection Agency of China has recommended that the total chromium concentration should be below 1.5 m L^{-1} and the Cr (VI) concentration should be below 0.5 m L^{-1} in integrated wastewater. Up to now, many treatment methods have been introduced such as ion exchange [6], chemical precipitation [7], electro-reduction [8], adsorption [2], photocatalytic reduction [9,10] and so on [11–13]. Among them, the adsorption is widely adopted to remove heavy metal ions from the wastewater, due to its low cost, ease operation and high efficiency. Therefore, preparing efficient adsorbents with excellent performance has become one of the principal challenges in the material chemistry and crystal engineering field and focus of interest of many researches.

Metal-organic framework (MOFs) have attracted considerable attentions owing to their large specific surface area, regular size and shape, abundant channel as well as excellent chemical and solvent stabilities [14–18]. A highly stable graphene-like 2D metal-organic framework (**BUC-17**) was synthesized under hydrothermal conditions by our research group [19], which exhibited ultrahigh uptake efficiency and capacity to Congo red (CR) due to its positive zeta potential. Based on the excellent adsorption performance of **BUC-17** toward anionic species, in this study, **BUC-17** was selected to accomplish adsorptive removal toward anionic Cr(VI). The involved kinetic models, isotherm models and the thermodynamic parameters were analyzed and calculated. Series experiments were designed to explore influencing factors of the adsorption process. As well, the possible adsorption mechanism was proposed, which was further affirmed by X-ray photoelectron spectra (XPS), scanning electron microscopy (SEM) and Fourier Transform infrared spectra (FTIR) analyses.

* Corresponding author.
E-mail address: wangchongchen@bucea.edu.cn (C.-C. Wang).

https://doi.org/10.1016/j.jece.2019.102909
Received 3 November 2018; Received in revised form 13 January 2019; Accepted 15 January 2019
Available online 16 January 2019

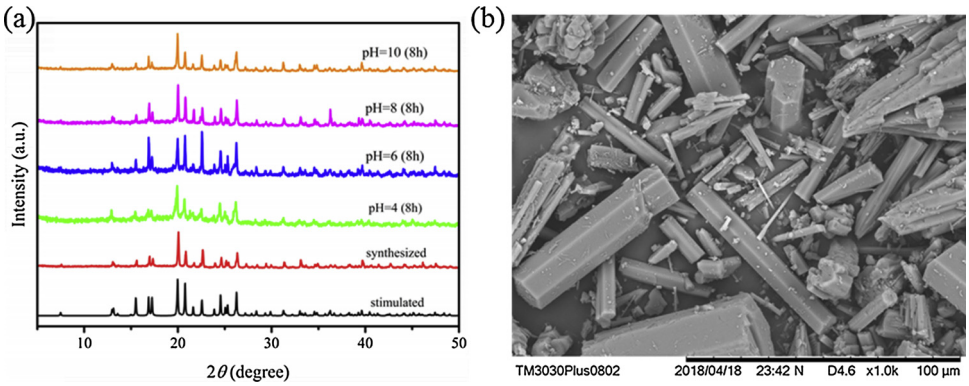

Fig. 1. (a) PXRD patterns of **BUC-17** before and after soaking, the simulated XRD pattern from single crystal structure of **BUC-17** and after adsorption; (b) SEM image of synthesized **BUC-17**.

2. Experimental

2.1. Materials and characterization

The reagent grade chemicals like cobaltous sulfate ($CoSO_4{\cdot}7H_2O$), 1,3-adamantanedicarboxylic acid (H_2adc), 1,3,5-tris(1-imidazolyl)benzene (tib), potassium dichromate ($K_2Cr_2O_7$) were commercially available and used directly without further purification.

Powder X-ray diffraction (PXRD) patterns of samples were assessed using a Dandonghaoyuan DX-2700B diffractometer with Cu Kα radiation, a step size of 0.02°, and a 2θ range of 5°–50°. Fourier Transform infrared spectra (FTIR) were performed using a Nicolet 6700 FTIR spectrophotometer in the region of 4000–400 cm^{-1} with KBr pellets. The surface charges of **BUC-17** at different pH values (4.0, 6.0, 8.0, 10.0) were recorded using the Malvern zeta sizer Nano ZS in the field strength of 20 V cm^{-1}. The pH value was adjusted using H_2SO_4 and NaOH solution. X-ray photoelectron spectra (XPS) measurement was carried out on a Thermo ESCALAB 250XI. A FEI Quanta 250 FEG scanning electron microscope (SEM) equipped with Bruker XFlash 5010 Energy Dispersive Spectrometer (EDS) was used to assess the morphology and the elemental mapping of **BUC-17**.

2.2. The preparation of $[Co_3(tib)_2(H_2O)_{12}](SO_4)_3$ (BUC-17) ultrafine powder

The **BUC-17** ultrafine powder was prepared according to the reported solvothermal procedure reported by Wang et al. with a minor modification [19]. A mixture of H_2adc (0.3 mmol, 0.0673 g), CoSO4·7H2O (0.3 mmol, 0.0843 g) and tib (0.3 mmol, 0. 0828 g) was sealed in a 25 mL Teflon-lined stainless steel Parr bomb containing deionized H2O (10 mL) and absolute ethanol (5 mL), heated at 413 K for 72 h, and then cooled down to room temperature. Red ultrafine powders of **BUC-17** were isolated and washed with deionized water and ethanol. The stability of **BUC-17** was examined by adding 20.0 mg **BUC-17** into 60 mL deionized water with various pH values from 4.0 to 10.0. The pH value was adjusted by using H_2SO_4 and NaOH solution with suitable concentration. The resulted suspension was stirred with 150 r min^{-1} at 298 K for 8 h. Finally, the solid sample was collected after filtration and drying processes for XRD test.

2.3. Adsorption performance of BUC-17 toward Cr(VI)

The adsorption performance of **BUC-17** was evaluated by the removal efficiency of Cr(VI) from the simulated wastewater prepared by adding 0.2829 g potassium dichromate of analytical grade to 1000 mL pure water. The experiments were conducted by adding certain dosages (250.0 mg L^{-1}) of **BUC-17** into 200 mL of 10 m L^{-1} Cr(VI) solution and stirring in water bath shaker with speed of 150 r min^{-1} at 298 K. During the adsorption reaction, 3.0 mL sample was extracted at regular intervals and separated from the adsorbent by centrifugation at 5000 rpm for 5 min. The residual Cr(VI) concentration in the supernatant was determined by dinitrodiphenyl carbazide spectrophotometric method under a Laspec Alpha-1860 spectrometer at 540 nm [20]. The adsorption amount was estimated using Eq. (1):

$$q = (C_0 - C_e)V/W \quad (1)$$

Where, q (mg g^{-1}) is the adsorption amount; C_0 and Ce (mg L^{-1}) are respectively the concentration of Cr(VI) at initial time and equilibrium time; V (L) is the volume of the Cr(VI) solution and W (g) is the dosage of adsorbent.

3. Results and discussion

3.1. Characterization of BUC-17

The powder XRD patterns of **BUC-17** matched well with the simulated ones from the single X-ray crystal structure date in Fig. 1(a), implying that **BUC-17** was in high purity. The PXRD patterns of **BUC-17** after being immerse in pure water with various pH values from 4.0 to 10.0 up to 8 h also completely fit well with those of the as-prepared **BUC-17**, indicating its excellent stability in acidic and alkaline environment. SEM images revealed that **BUC-17** exhibits the stick-like shape and regular morphology, as displayed in Fig. 1(b).

3.2. Adsorption performance

3.2.1. Adsorption kinetics

The adsorption kinetic experiment was performed by mixing certain dosages (250.0 mg L^{-1}) of **BUC-17** and 200 mL Cr(VI) solution with pH = 4.0 with concentrations ranging from 25 mg L^{-1} to 35 mg L^{-1} and stirring for 8 h in water bath shaker with speed of 150 r min^{-1} at 298 K. The pseudo-first-model [21] and pseudo-second-model [21] expressed as Eqs. (2) and (3) were utilized to describe the adsorption process in this study, respectively.

$$\ln(q_e - q_t) = \ln(q_e) - k_1 t \quad (2)$$

$$\frac{t}{q_t} = \frac{1}{k_2 q_e^2} + \frac{1}{q_e} t \quad (3)$$

Where, q_t and q_e (mg g^{-1}) are respectively the masses of Cr(VI) adsorbed per unit mass of the sorbent at a certain time t and equilibrium time; k_1 (min^{-1}) and k_2 (g mg^{-1} min^{-1}) represent the pseudo first-order adsorption rate constant and the pseudo-first-order adsorption rate constant, respectively (Table 1).

Furthermore, the data were also tested by Weber–Morris model expressed as Eq. (4) [22] to investigate the existence of intra-particle diffusion in the adsorption process.

Table 1
The adsorption capacity comparison of some typical adsorbents toward Cr(VI).

Adsorbents	Adsorption capacity (mg g^{-1})	Equilibrium time	Refs.
IL-MIL-100(Fe)	285.7	5 h	[28]
ZJU-101	245	10 min	[29]
MP@ZIF-8	136.56	16 h	[30]
UiO-66-HA	129	NA	[31]
MOF-867	53.4	12 h	[29]
ZIF-67	15.43	60 min	[32]
ZIF-8	0.15	60 min	[33]
BUC-17	121	8 h	This work

$$Q_t = kt^{0.5} + C \quad (4)$$

Where, k (mg g^{-1} $min^{-0.5}$) is the rate constant of intra-particle diffusion.

The Cr(VI) adsorption process as a function of time was examined. The results indicated that the Cr(VI) adsorbed amount increased with the increase of contact time, and Cr(VI) was removed very fast in the first 4 h and the Cr(VI) adsorption increased slowly until the equilibrium time. The adsorption equilibrium was reached around 8 h and the Cr(VI) adsorption capacity was attained 121 mg g^{-1}. Comparing to some adsorbents as listed in Table 1, **BUC-17** exhibited good adsorption activity toward Cr(VI) in relatively short time [23]. In recent years, adsorption kinetics included the pseudo-first-order model and the pseudo-second-order model have been widely applied to the adsorption mechanism of pollutants from aqueous solutions onto adsorbents [24]. From the kinetic parameters of the above-stated models in Table 2 , it can be seen that the pseudo-second-order model was fitted well to the kinetic data, implying that the rate-limiting step might be chemisorption [25]. Furthermore, the linear portion of plot is not passing through the origin (Fig. S1 in the ESI), which indicates that the mechanism of Cr (VI) adsorption on **BUC-17** is complex procedure and intra-particle diffusion is not the only control step in the adsorption process. It has been found that surface adsorption as well as intra-particle diffusion contributes to the rate determining step [26,27].

3.2.2. Adsorption isotherms

To study the effect of temperature, the adsorption isotherms experiment was demonstrated by mixing certain dosages (250.0 mg L^{-1}) of **BUC-17** and 200 mL Cr(VI) solution with pH = 4.0 with initial concentration of 20, 25, 30, 35, 40 mg L^{-1}. The mixtures were respectively stirred in constant temperature water bath shaker with speed of 150 r min^{-1} at different temperatures (293, 298 and 303 K).

The Langmuir, Freundlich, and Dubinin–Radushkevich (D-R) adsorption isotherm models are widely used to describe the equilibrium relationship between the adsorbent and the adsorbate, the affinity and the adsorption capacity of the adsorbent.

The Langmuir isotherm model can be represented as Eq. (5) [34]:

$$C_e/q_e = 1/K_L q_{max} + C_e/q_{max} \quad (5)$$

Where, q_{max} (mg g^{-1}) is the maximum amount of adsorption with complete monolayer coverage on the adsorbent surface; K_L is the Langmuir constant related to the energy of adsorption in L mg^{-1}.

The Freundlich isotherm model can be expressed as Eq. (6) [35]:

$$\log q_e = \log K_f + (1/n)\log C_e \quad (6)$$

Where, n represents the degree of nonlinearity between solution concentration and adsorption; K_f (mg g^{-1}) is the Freundlich adsorption isotherm constants which indicated the extent of the adsorption.

The Dubinin–Radushkevich (D-R) isotherm model is generally listed in Eq. (7) [36]:

$$\ln q_e = \ln q_m - K_{DR}\varepsilon^2 \quad (7)$$

Where, qm (mol g^{-1}) represents the theoretical saturation capacity, K_{DR} (mol^2 J^{-2}) is the activity coefficient related to mean sorption energy; ε (J mol^{-1}) and E (kJ mol^{-1}) mean the potential and free energy of adsorption, respectively. They can be respectively calculated using Eqs. (8) and (9):

$$\varepsilon = RT\ln(1+1/C_e) \quad (8)$$

$$E = \frac{1}{\sqrt{2K_{DR}}} \quad (9)$$

To clarify the detailed adsorption mechanism of **BUC-17** toward Cr (VI), the adsorption isotherms were calculated as shown in Table 3. It can be seen that the obtained R^2 values for the Langmuir model are above 0.99 at different temperatures, indicating the adsorption of **BUC-17** toward Cr(VI) was suitably fitted to the Langmuir model, similar to **BUC-17** in the previous reports [19]. Thus, the adsorption toward Cr (VI) is chemisorption as well as monolayer sorption on a surface [37]. The amount of adsorbed Cr(VI) increased with temperatures, implying that the adsorption of Cr(VI) as an endothermic reaction was favorable at high temperatures. Moreover, the value of adsorption intensity decreasing from 0.0540 to 0.0388 is less than unity, which manifests favorable in the adsorption process [38].

3.2.3. Thermodynamic parameters

Thermodynamic parameters including standard free energy (ΔG°, kJ mol^{-1}), change in enthalpy (ΔH°, kJ mol^{-1}) and change in entropy (ΔS°, J mol^{-1} K^{-1}), were determined with the aid of date obtained from Langmuir adsorption isotherm via Eqs. (10) and (11) [39]:

$$\Delta G^0 = -RT\ln K_L \quad (10)$$

$$\ln K_L = \frac{\Delta S^0}{R} - \frac{\Delta H^0}{RT} \quad (11)$$

Where, R (8.314 kJ mol^{-1} K^{-1}) is the universal gas constant and T (K) is the absolute temperature, K_L is equilibrium constant, which depends on the temperature.

To further establish the thermodynamic function, the possible driving forces and even the mechanism of the sorption process, the standard free energy ΔG°, enthalpy ΔH°, and entropy ΔS° were calculated founded on the date obtained from the Langmuir adsorption isotherm, as illustrated in Table 4. Generally, the free energy ΔG° values ranging from −20 to 0 kJ mol^{-1} signifies a physi-sorption process, while ΔG° values between −80 and −400 kJ mol^{-1} indicates that chemisorption process is dominated [40]. In this study, the ΔG° values between −37.90 and −39.50 kJ mol^{-1}, indicated that the adsorption process was chiefly controlled by physical adsorption along with partial chemical adsorption [40,41]. Moreover, the negative values of all ΔG° implied that the sorption process was spontaneous in nature and favorable at higher temperature [42,43], which might also be confirmed from the maximum adsorption capacity of **BUC-17** increase from

Table 2
Parameters of kinetic model of Cr(VI) with different concentration onto **BUC-17** (298 K).

	Pseudo-first-order			Pseudo-second-order			Experimental value (mg g^{-1})
C_0 (mg L^{-1})	k_1 (min^{-1})	q_e (mg g^{-1})	R^2	K_2 (g mg^{-1} min^{-1})	q_e (mg g^{-1})	R^2	
35	0.0046	67.65	0.748	1.84×10^{-4}	97.09	0.970	92.59
30	0.0090	48.75	0.892	4.50×10^{-4}	74.63	0.999	71.17
25	0.0134	46.84	0.961	5.77×10^{-3}	68.03	0.999	64.36

Table 3
Constants of Langmuir, Freundich, and D–R for Cr(VI) adsorption by **BUC-17** at different temperatures.

T/K	Langmuir			Freundlich			D-R		
	q_{max}(mg g^{-1})	K_L(L mg^{-1})	R^2	K_f (L g^{-1})	1/n	R^2	K_{DR}	E(KJ mol^{-1})	R^2
293	76.34	11.9	0.998	6.62	0.0540	0.481	2×10^{-7}	1.58	0.811
298	80.65	12.4	0.996	68.61	0.0697	0.483	1×10^{-7}	2.24	0.816
303	82.64	13.4	0.999	75.44	0.0388	0.711	4×10^{-8}	3.54	0.973

Table 4
Thermodynamic parameters for Cr(VI) adsorption by **BUC-17** at different temperatures.

T/K	K_L (L mg^{-1})	$\Delta G°$ (kJ mol^{-1})	$\Delta S°$ (J mol^{-1} K^{-1})	$\Delta H°$ (kJ mol^{-1})
293	5715609	−37.90	159.69	8.90
298	5950760	−38.65		
303	6449856	−39.50		

76.34 mg g^{-1} at 293 K to 82.64 mg g^{-1} at 303 K. On the other hand, the average enthalpy $\Delta H°$ and entropy $\Delta S°$ of the process have been respectively evaluated as 8.90 kJ mol^{-1} and 159.69 J mol^{-1} K^{-1}. The positive value of $\Delta H°$ demonstrates that the endothermic nature of the sorption process [44], while the positive value of $\Delta S°$ suggests the randomness increased during the adsorption process [45].

3.3. Influencing factors

3.3.1. Influence of pH

The adsorption capacity of **BUC-17** toward Cr(VI) at natural pH was firstly investigated, certain dosages (250.0 mg L^{-1}) of **BUC-17** was added to 200 mL solutions containing 10 mg L^{-1} of Cr(VI) solution with various pH values. The initial pH values were adjusted from 4.0 to 10.0 using H_2SO_4 and NaOH aqueous solution with suitable concentration, respectively. As shown in Fig. 2(a), it is evident that the adsorption capacity of the adsorbent decreases from 47.4 to 0.5 mg g^{-1} as the pH value increases from 4.0 to 10.0. It was revealed that the pH value plays an important role in the removal of Cr(VI) in the solution [2,46]. In this system, the sorbent is positively charged, which was confirmed by the examined zeta potential ranging from 16.4 to 23.8 mV as the pH value as illustrated in Fig. 2(b). Meanwhile, it is well known that the dominant form of Cr(VI) in nature is anionic species like $HCrO_4$-, CrO_4^{2-} and $Cr_2O_7^{2-}$ [47–49]. Thus, its adsorption performance toward Cr(VI) might be attributed to the electrostatic interactions between anionic Cr(VI) species and positive surface of **BUC-17**. Cr(VI) exists mainly as $HCrO_4$- and $Cr_2O_7^{2-}$ oxyanions under the condition of pH < 7; However, for pH > 7, CrO_4^{2-} was the primary species in the solution [48,50,51]. The zeta potential of **BUC-17** decreased with the further increase of pH, which leads to the gradually decreased area occupied by the average single Cr(VI) adsorption, and finally resulting in the much lower adsorption performance. Under higher pH, the zeta potential of **BUC-17** was further decreased and the formed CrO_4^{2-} will occupy more active area [51], which contributed to the declined adsorption performance toward Cr(VI) [48,52]. On the other hand, the declined adsorption activity as the increasing concentration of OH^- may also be due to the higher competition for the positively charged sites between OH^- anions and Cr(VI) [2,48].

3.3.2. Influence of adsorbent dosage and initial Cr(VI) concentration

The influence of Cr(VI) removal was affected by the adsorbent dosage and initial Cr(VI) ions concentration. Certain dosages (150.0 mg L^{-1}, 250.0 mg L^{-1}, 350.0 mg L^{-1}) of **BUC-17** were agitated with 200 mL Cr(VI) solution with initial concentration of 5, 10, 15 mg L^{-1} with pH = 4.0. As shown in Fig. 3a, when the adsorbent dosage increased from 150.0 to 350.0 mg L^{-1}, the adsorbed Cr(VI) amount decreased from 68.2 mg g^{-1} to 41.2 mg g^{-1}, which can be ascribed to the active sites on the surface of the adsorbate could be occupied sufficiently. The increase of initial Cr(VI) concentration led to significant decrease of removal percentage (Fig. 3b). The blockage of adsorption sites inside the MOF **BUC-17** crystals were occupied by immediate surface adsorption of Cr(VI) ions, thus preventing further access of the Cr(VI) ions into the interior cages of the MOF **BUC-17**, which resulted in the observed drop of Cr(VI) removal percentage while still maintained increased overall removal performance of Cr(VI) ions.

3.3.3. Influence of coexistence anion

The influence of coexisting anions on Cr(VI) adsorption was examined by adding certain dosages (350.0 mg L^{-1}) of **BUC-17** into 200 mL of 15 mg L^{-1} Cr(VI) solution with and without coexistent anions (SO_4^{2-}, NO_3^-, Cl^-, PO_4^{3-}). The concentration of each coexisting anion was 1.5 mmol L^{-1}, and the concentration of all coexistent anions was 10 times higher than that of Cr(VI) ion. Generally, some co-existed anions always exist in real industry waste water [53]. As shown in Fig.4, the presence of inorganic anions (Cl^-, NO_3^-, SO_4^{2-}, PO_4^{3-}) has negative effect on the process of adsorption of Cr(VI) by **BUC-17**, which may be due to their competitive sorption based on the electrostatic interaction. The effect of inorganic anions on adsorption is as follows: $Cl^- < NO_3^- < SO_4^{2-} < PO_4^{3-}$. Moreover, the pH value is greatly increased after adding PO_4^{3-} to the solution (in the experiment, the

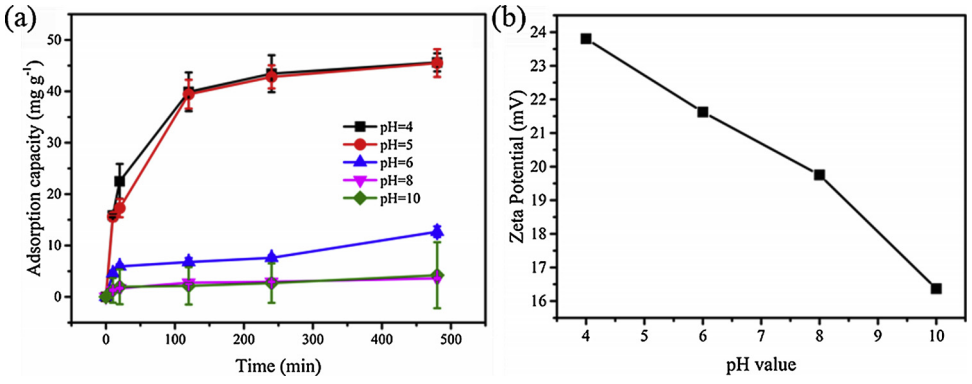

Fig. 2. (a) The adsorption capacity of **BUC-17** at different pHs; (b) the zeta potential of **BUC-17**.

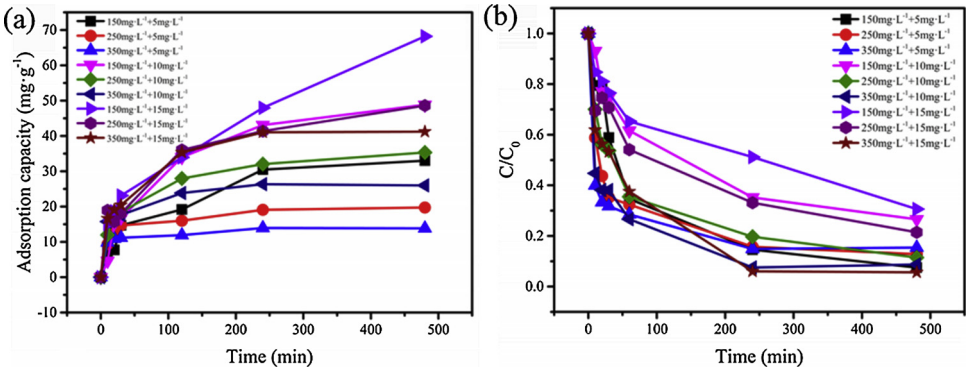

Fig. 3. (a) The adsorption capacity and (b) the removal percentage of **BUC-17** at different adsorbent dosages and initial Cr(VI) concentrations.

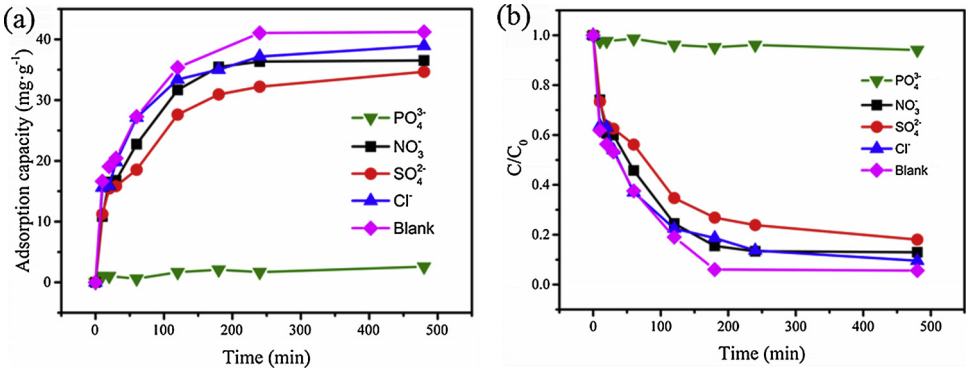

Fig. 4. (a) The adsorption capacity and (b) the removal percentage of **BUC-17** with addition of inorganic salts.

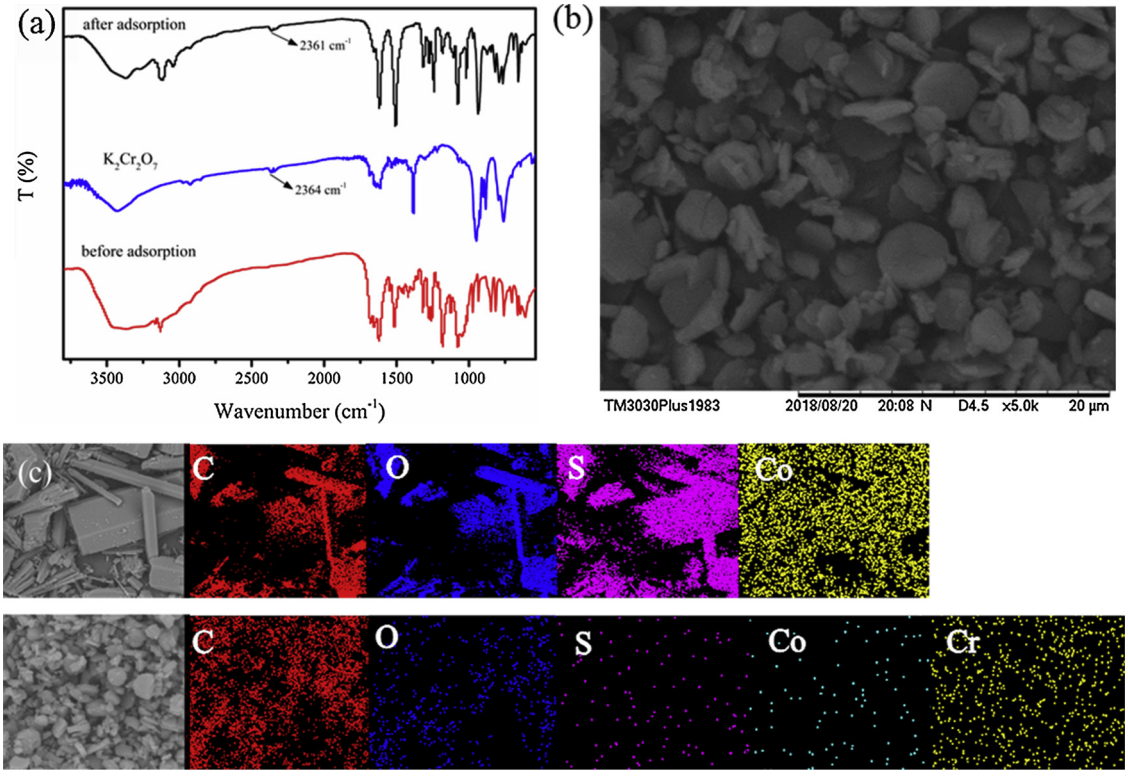

Fig. 5. (a) the FTIR spectra of potassium dichromate, **BUC-17** before and after adsorption; (b) SEM of **BUC-17** after adsorption; (c) Elemental mapping of **BUC-17** before and after adsorption.

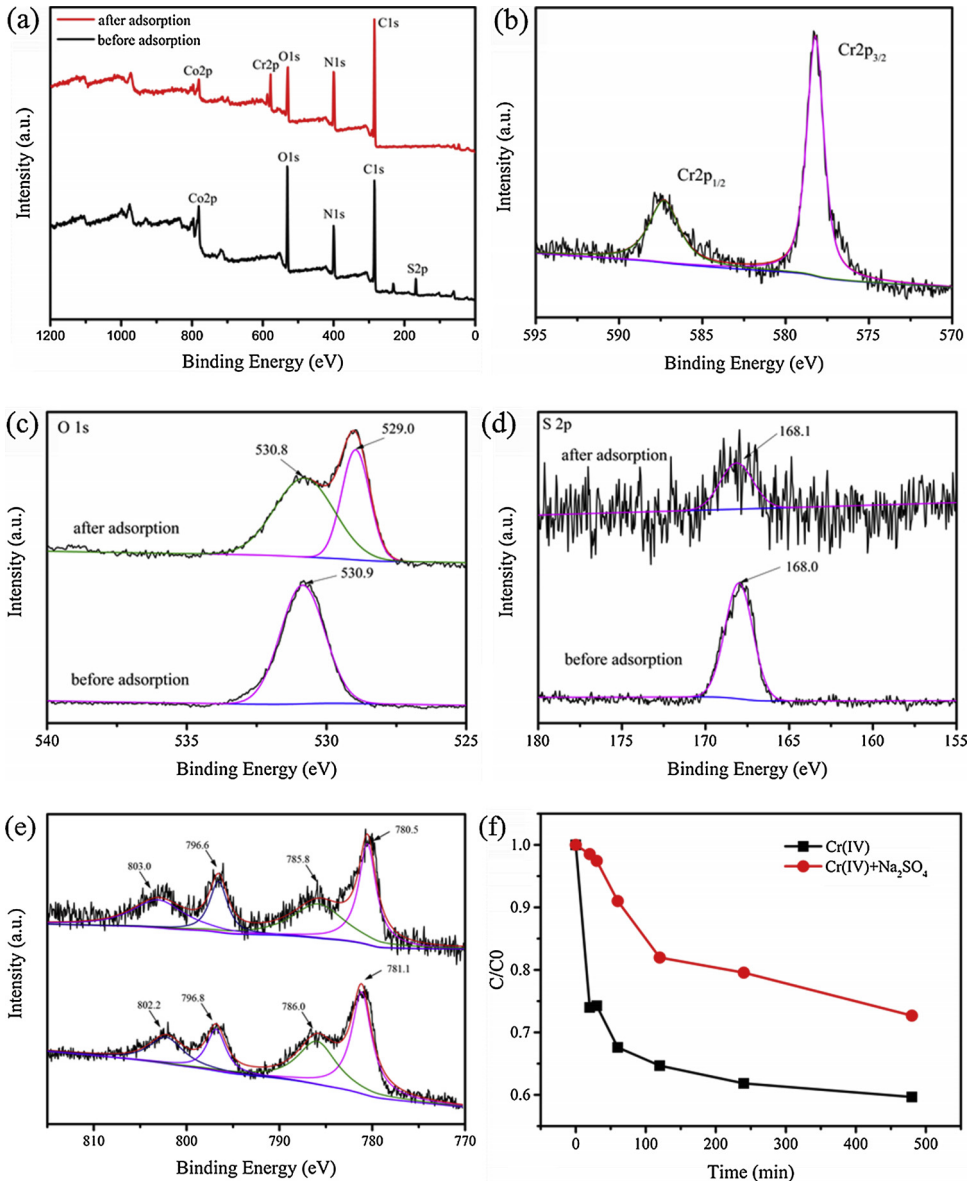

Fig. 6. (a) Full range XPS spectra of **BUC-17** before and after adsorption of Cr(VI); (b) XPS spectra of Cr 2p before and after adsorption of Cr(VI); (c) XPS spectra of O 1s before and after adsorption of Cr(VI); (d) XPS spectra of S 2p before and after adsorption of Cr(VI); (e) XPS spectra of Cr 2p before and after adsorption of Cr(VI); (f) Adsorption of Cr(IV) in deionized water and in saturated Na_2SO_4 solution with **BUC-17**.

addition of PO_4^{3-} resulted in solution pH increases from 4.0 to 8.9), which also leads to a decrease in the amount of adsorption.

3.4. Proposed adsorption mechanism

To verify the adsorption of Cr(VI) onto **BUC-17**, the FTIR spectra and the mapping of **BUC-17** were studied. As shown in Fig. 5(a) and (b), in FTIR spectra, a new adsorption band at 2361 cm^{-1} of **BUC-17** after adsorption appeared, which confirmed the adsorption of Cr(VI) onto **BUC-17**. The elemental mapping obtained from SEM verified that the presence of Cr in **BUC-17** after adsorbing Cr(VI) besides C, N,O, S and Co in the as-prepared **BUC-17** as demonstrated in Fig. 5(c) and (d). Moreover, the adsorption of Cr(VI) onto **BUC-17** was also confirmed by XPS, in which the XPS spectra signals of Cr with binding energy of 578.2 (Cr 2p) could be detected [54], as shown in Fig. 6(b). Furthermore, both the SEM image and PXRD patterns of **BUC-17** after adsorption matched well with the corresponding ones of as-prepared **BUC-17**, which further affirmed **BUC-17** was stable during the adsorption process, as depicted in Figs. 1 and 5.

According to previously reported the properties of **BUC-17** by Li et al. [19], **BUC-17** was preferred to capture anionic dyes due to its positive surface charge. Therefore, the uptake of Cr(VI) via **BUC-17** as absorbent was attributed to electrostatic interaction, as confirmed by an overall positive surface charge of **BUC-17** from pH = 4 to pH = 10 illustrated in Fig. 2(b). Besides, the uncoordinated SO_4^{2-} in the **BUC-17** structure was proposed to be exchanged with the Cr(VI) ions during sorption, which was confirmed by its adsorption performance toward Cr (VI) in saturated aqueous Na_2SO_4 solution and in pure aqueous solution. These result revealed that the presence of SO_4^{2-} obviously inhibited the adsorption Cr(VI) onto **BUC-17**, as evidenced by the adsorption efficiency decrease from 40.3% (in pure aqueous solution) to 27.3% (in saturated aqueous Na_2SO_4 solution) within 8 h, as shown in Fig. 6(e). To further illustrate the adsorption mechanism, XPS was used for analysis of adsorption mechanism as illustrated in Fig. 6, in which the S 2p peak of SO_4^{2-} from **BUC-17** disappeared and new Cr 2p (578.2 eV and 587.3 eV) peaks belonging to $Cr_2O_7^{2-}$ emerged after adsorption [54,55], implying that ion-exchange interactions contribute to Cr(VI) adsorption on **BUC-17** [56,57]. Meanwhile, the elemental

mapping obtained from SEM revealed the existence of S and Co (the characteristics element of **BUC-17**) made no change in oxidation state occurred after adsorbing Cr(VI) [58].

4. Conclusion

In all, it is successful to produce **BUC-17** ultrafine powder via the introduction of absolute ethanol, which exhibited ultra-high adsorption capacity towards Cr(VI) (121 mg Cr(VI) per gram of **BUC-17**). The adsorption capacity of **BUC-17** towards Cr(VI) was much more than most of the adsorbents reported previously. The adsorption process fitted well with pseudo-second-order kinetic model as well as Langmuir isotherms, which demonstrated that the corresponding adsorption process was spontaneous, endothermic and the randomness increases. The overall data presented in this study indicated that both electrostatic and ion-exchange interactions contribute to Cr(VI) adsorption onto **BUC-17**. Moreover, experimental data revealed that co-exiting anions and pH played important roles in the adsorption process. It was expected to use **BUC-17** as efficient adsorbent to remove anionic heavy metals from wastewater.

Acknowledgements

The authors acknowledge financial support from the National Natural Science Foundation of China (51578034), Great Wall Scholars Training Program Project of Beijing Municipality Universities (CIT& TCD20180323), Project of Construction of Innovation Teams and Teacher Career Development for Universities and Colleges Under Beijing Municipality (IDHT20170508), Beijing Talent Project (2018A35), Scientific Research Foundation of Beijing University of Civil Engineering and Architecture (KYJJ2017008), and the Fundamental Research Funds for Beijing University of Civil Engineering and Architecture (X18276).

Appendix A. Supplementary data

Supplementary material related to this article can be found, in the online version, at doi:https://doi.org/10.1016/j.jece.2019.102909.

References

[1] C. Camara, R. Cornelis, P. Quevauviller, Assessment of methods currently used for the determination of Cr and Se species in solutions, Trends Anal. Chem. 19 (2000) 189–194.
[2] A.K. Bhattacharya, T.K. Naiya, S.N. Mandal, S.K. Das, Adsorption, kinetics and equilibrium studies on removal of Cr(VI) from aqueous solutions using different low-cost adsorbents, Chem. Eng. J. 137 (2008) 529–541.
[3] X.-D. Du, X.-H. Yi, P. Wang, W. Zheng, J. Deng, C.-C. Wang, Robust photocatalytic reduction of Cr(VI) on UiO-66-NH2(Zr/Hf) metal-organic framework membrane under sunlight irradiation, Chem. Eng. J. 356 (2019) 393–399.
[4] X. Zhang, L. Lv, Y. Qin, M. Xu, X. Jia, Z. Chen, Removal of aqueous Cr(VI) by a magnetic biochar derived from Melia azedarach wood, Bioresour. Technol. 256 (2018) 1–10.
[5] K. Selvi, S. Pattabhi, K. Kadirvelu, Removal of Cr(VI) from aqueous solution by adsorption onto activated carbon, Bioresour. Technol. 80 (2001) 87–89.
[6] G. Tiravanti, D. Petruzzelli, R. Passino, Pretreatment of tannery wastewaters by an ion exchange process for Cr(III) removal and recovery, Water Sci. Technol. 36 (1997) 197–207.
[7] X. Zhou, T. Korenaga, T. Takahashi, T. Moriwake, S. Shinoda, A process monitoring/controlling system for the treatment of wastewater containing chromium (VI), Water Res. 27 (1993) 1049–1054.
[8] L.A.M. Ruotolo, J.C. Gubulin, Optimization of Cr(VI) electroreduction from synthetic industrial wastewater using reticulated vitreous carbon electrodes modified with conducting polymers, Chem. Eng. J. 149 (2009) 334–339.
[9] X.-H. Yi, F.-X. Wang, X.-D. Du, H. Fu, C.-C. Wang, Highly efficient photocatalytic Cr (VI) reduction and organic pollutants degradation of two new bifunctional 2D Cd/Co-based MOFs, Polyhedron 152 (2018) 216–224.
[10] F.X. Wang, X.H. Yi, C.C. Wang, J.G. Deng, Photocatalytic Cr(VI) reduction and organic-pollutant degradation in a stable 2D coordination polymer, Chin. J. Catal. 38 (2017) 2141–2149.
[11] C.C. Wang, X.D. Du, J. Li, X.X. Guo, P. Wang, J. Zhang, Photocatalytic Cr(VI) reduction in metal-organic frameworks: a mini-review, Appl. Catal. B: Environ. 193 (2016) 198–216.
[12] C.E. Barrera, A review of chemical, electrochemical and biological methods for aqueous Cr(VI) reduction, J. Hazard. Mater. 223–224 (2012) 1–12.
[13] A.K. Chakravarti, S.B. Chowdhury, Liquid membrane multiple emulsion process of chromium(VI) separation from waste waters, Colloids Surf. A: Physicochem. Eng. Asp. 103 (1995) 59–71.
[14] E. Haque, J.W. Jun, S.H. Jhung, Adsorptive removal of methyl orange and methylene blue from aqueous solution with a metal-organic framework material, iron terephthalate (MOF-235), J. Hazard. Mater. 185 (2011) 507–511.
[15] C.C. Wang, Y.S. Ho, Research trend of metal—organic frameworks: a bibliometric analysis, Scientometrics 109 (2016) 1–33.
[16] C.C. Wang, J.R. Li, X.L. Lv, Y.Q. Zhang, G. Guo, Photocatalytic organic pollutants degradation in metal–organic frameworks, Energy Environ. Sci. 7 (2014) 2831–2867.
[17] F.X. Wang, C.C. Wang, P. Wang, B.C. Xing, Syntheses and applications of UiO series of MOFs, Chin. J. Inorg. Chem. 33 (2017) 713–737.
[18] X.-Y. Xu, C. Chu, H. Fu, X.-D. Du, P. Wang, W. Zheng, C.-C. Wang, Light-responsive UiO-66-NH2/Ag3PO4 MOF-nanoparticle composites for the capture and release of sulfamethoxazole, Chem. Eng. J. 350 (2018) 436–444.
[19] J.J. Li, C.C. Wang, H.F. Fu, J.R. Cui, P. Xu, J. Guo, J.R. Li, High-performance adsorption and separation of anionic dyes in water using a chemically stable graphene-like metal-organic framework, Dalton Trans. 46 (2017) 10197–10201.
[20] R. Milačič, J. Štupar, N. Kožuh, J. Korošin, Critical evaluation of three analytical techniques for the determination of chromium(VI) in soil extracts, Analyst 117 (1992) 125–130.
[21] Y.S. Ho, A.E. Ofomaja, Pseudo-second-order model for lead ion sorption from aqueous solutions onto palm kernel fiber, J. Hazard. Mater. 129 (2006) 137–142.
[22] W.J. Weber, J.C. Morris, Intraparticle diffusion during the sorption of surfactants onto activated carbon, J. Sanit. Eng. Division Am. Soc. Civ. Eng. 89 (1963) 53–61.
[23] M. Feng, P. Zhang, H.-C. Zhou, V.K. Sharma, Water-stable metal-organic frameworks for aqueous removal of heavy metals and radionuclides: a review, Chemosphere 209 (2018) 783–800.
[24] Y.S. Ho, Review of second-order models for adsorption systems, J. Hazard. Mater. 37 (2006) 681–689.
[25] X. Zhao, Y. Wei, H. Zhao, Z. Gao, Y. Zhang, L. Zhi, Y. Wang, H. Huang, Functionalized metal-organic frameworks for effective removal of rocephin in aqueous solutions, J. Colloid Interface Sci. 514 (2017) 234–239.
[26] X. Zhao, D. Liu, H. Huang, W. Zhang, Q. Yang, C. Zhong, The stability and defluoridation performance of MOFs in fluoride solutions, Microporous Mesoporous Mater. 185 (2014) 72–78.
[27] M. Mahramanlioglu, I. Kizilcikli, I.O. Bicer, Adsorption of fluoride from aqueous solution by acid treated spent bleaching earth ☆, J. Fluor. Chem. 115 (2002) 41–47.
[28] A. Nasrollahpour, S.E. Moradi, Hexavalent chromium removal from water by ionic liquid modified metal-organic frameworks adsorbent, Microporous Mesoporous Mater. 243 (2017) 47–55.
[29] Q. Zhang, J. Yu, J. Cai, L. Zhang, Y. Cui, Y. Yang, B. Chen, G. Qian, A porous Zr-cluster-based cationic metal–organic framework for highly efficient Cr2O72− removal from water, Chem. Commun. 51 (2015) 14732–14734.
[30] K. Zhu, C. Chen, H. Xu, Y. Gao, X. Tan, A. Alsaedi, T. Hayat, Cr(VI) Reduction and Immobilization by core-double-shell structured magnetic polydopamine@Zeolitic idazolate frameworks-8 microspheres, ACS Sustain. Chem. Eng. 5 (2017) 6795–6802.
[31] Sofia Rapti, Anastasia Pournara, Debajit Sarma, Ioannis T. Papadas, Gerasimos S. Armatas, Athanassios C. Tsipis, Theodore Lazarides, Mercouri G. Kanatzidis, Manolis J. Manos, Selective capture of hexavalent chromium from an anion-exchange column of metal organic resin-alginic acid composite, Chem. Sci. 7 (2016) 2438-2438.
[32] X. Li, X. Gao, L. Ai, J. Jiang, Mechanistic insight into the interaction and adsorption of Cr(VI) with zeolitic imidazolate framework-67 microcrystals from aqueous solution, Chem. Eng. J. 274 (2015) 238–246.
[33] M. Niknam Shahrak, M. Ghahramaninezhad, M. Eydifarash, Zeolitic imidazolate framework-8 for efficient adsorption and removal of Cr(VI) ions from aqueous solution, Environ. Sci. Pollut. Res. 24 (2017) 9624–9634.
[34] I. Langmuir, Constitution and fundamental properties of solids and liquids: I, solids, J. Am. Chem. Soc. 183 (1916) 102–105.
[35] M. Kumar, R. Tamilarasan, V. Sivakumar, Adsorption of victoria blue by carbon/Ba/alginate beads: kinetics, thermodynamics and isotherm studies, Carbohydr. Polym. 98 (2013) 505–513.
[36] E. Eren, Removal of basic dye by modified Unye bentonite, Turkey, J. Hazard. Mater. 162 (2009) 1355–1363.
[37] N. Viswanathan, S. Meenakshi, Enhanced fluoride sorption using La(III) incorporated carboxylated chitosan beads, J. Colloid Interface Sci. 322 (2008) 375–383.
[38] N. Chen, Z. Zhang, C. Feng, D. Zhu, Y. Yang, N. Sugiura, Preparation and characterization of porous granular ceramic containing dispersed aluminum and iron oxides as adsorbents for fluoride removal from aqueous solution, J. Hazard. Mater. 186 (2011) 863–868.
[39] Y. Bulut, Z. Tez, Adsorption studies on ground shells of hazelnut and almond, J. Hazard. Mater. 149 (2007) 35–41.
[40] X.-D. Du, C.-C. Wang, J. Zhong, J.-G. Liu, Y.-X. Li, P. Wang, Highly efficient removal of Pb2+ by a polyoxomolybdate-based organic-inorganic hybrid material {(4-Hap)4[Mo8O26]}, J. Environ. Chem. Eng. 5 (2017) 1866–1873.
[41] A. Mittal, D. Jhare, J. Mittal, V.K. Gupta, Batch and bulk removal of hazardous colouring agent rose bengal by adsorption over bottom ash, RSC Adv. 2 (2012) 8381–8389.
[42] A. Sari, M. Tuzen, D. Citak, M. Soylak, Equilibrium, kinetic and thermodynamic studies of adsorption of Pb(II) from aqueous solution onto Turkish kaolinite clay, J.

Hazard. Mater. 149 (2007) 283–291.
[43] A.B. Zaki, M.Y. El-Sheikh, J. Evans, S.A. El-Safty, Kinetics and mechanism of the sorption of some aromatic amines onto amberlite IRA-904 anion-exchange resin, J. Colloid Interface Sci. 221 (2000) 58–63.
[44] A. Mittal, D. Jhare, J. Mittal, Adsorption of hazardous dye Eosin Yellow from aqueous solution onto waste material De-oiled Soya: isotherm, kinetics and bulk removal, J. Mol. Liq. 179 (2013) 133–140.
[45] A. Özcan, A.S. Özcan, S. Tunali, T. Akar, I. Kiran, Determination of the equilibrium, kinetic and thermodynamic parameters of adsorption of copper(II) ions onto seeds of Capsicum annuum, J. Hazard. Mater. 124 (2005) 200–208.
[46] M. Kobya, Removal of Cr(VI) from aqueous solutions by adsorption onto hazelnut shell activated carbon: kinetic and equilibrium studies, Bioresour. Technol. 91 (2004) 317–321.
[47] C. Raji, T.S. Anirudhan, Batch Cr(VI) removal by polyacrylamide-grafted sawdust: kinetics and thermodynamics, Water Res. 32 (1998) 3772–3780.
[48] M. Gheju, I. Balcu, G. Mosoarca, Removal of Cr(VI) from aqueous solutions by adsorption on MnO2, J. Hazard. Mater. 310 (2016) 270–277.
[49] A.A. Taha, Y.N. Wu, H. Wang, F. Li, Preparation and application of functionalized cellulose acetate/silica composite nanofibrous membrane via electrospinning for Cr (VI) ion removal from aqueous solution, J. Environ. Manage. 112 (2012) 10–16.
[50] M. Gheju, Hexavalent chromium reduction with zero-valent Iron (ZVI) in aquatic systems, Water Air Soil Pollut. 222 (2011) 103–148.
[51] D. Zhao, S.G. And, L. Stewart, Selective removal of Cr(VI) oxyanions with a new anion exchanger, Ind. Eng. Chem. Res. 37 (1998) 4383–4387.
[52] S. Rapti, D. Sarma, S.A. Diamantis, E. Skliri, G.S. Armatas, A.C. Tsipis, Y.S. Hassan, M. Alkordi, C.D. Malliakas, M.G. Kanatzidis, T. Lazarides, J.C. Plakatouras, M.J. Manos, All in one porous material: exceptional sorption and selective sensing of hexavalent chromium by using a Zr4+ MOF, J. Mater. Chem. A 5 (2017) 14707–14719.
[53] W.A. El-Mehalmey, A.H. Ibrahim, A.A. Abugable, M.H. Hassan, R.R. Haikal, S.G. Karakalos, O. Zaki, M.H. Alkordi, Metal–organic framework@silica as a stationary phase sorbent for rapid and cost-effective removal of hexavalent chromium, J. Mater. Chem. A 6 (2018) 2742–2751.
[54] B.A. Manning, J.R. Kiser, H. Kwon, S.R. Kanel, Spectroscopic investigation of Cr (III)- and Cr(VI)-treated nanoscale zerovalent iron, Environ. Sci. Technol. 41 (2007) 586–592.
[55] G. Cappelletti, C.L. Bianchi, S. Ardizzone, Nano-titania assisted photoreduction of Cr(VI): the role of the different TiO2 polymorphs, Appl. Catal. B: Environ. 78 (2008) 193–201.
[56] K. Sutthiumporn, S. Kawi, Promotional effect of alkaline earth over Ni–LaO catalyst for CO reforming of CH: role of surface oxygen species on H production and carbon suppression, Int. J. Hydrogen Energy 36 (2011) 14435–14446.
[57] X.-X. Song, H. Fu, P. Wang, H.-Y. Li, Y.-Q. Zhang, C.-C. Wang, The selectively fluorescent sensing detection and adsorptive removal of Pb2+ with a stable [δ-Mo8O26]-based hybrid, J. Colloid Interface Sci. 532 (2018) 598–604.
[58] A. Liu, C.-C. Wang, C.-z. Wang, H.-f. Fu, W. Peng, Y.-L. Cao, H.-Y. Chu, A.-F. Du, Selective adsorption activities toward organic dyes and antibacterial performance of silver-based coordination polymers, J. Colloid Interface Sci. 512 (2018) 730–739.